
Recursive Two-Step Lookahead Expected Payoff for Time-Dependent Bayesian Optimization

S. Ashwin Renganathan

Mathematics & Computer Sciences
Argonne National Laboratory
Lemont, IL 60439
srenganathan@anl.gov

Jeffrey Larson

Mathematics & Computer Sciences
Argonne National Laboratory
Lemont, IL 60439
jmlarson@anl.gov

Stefan Wild

Mathematics & Computer Sciences
Argonne National Laboratory
Lemont, IL 60439
wild@anl.gov

Abstract

We propose a novel Bayesian method to solve the maximization of a time-dependent expensive-to-evaluate oracle. We are interested in the decision that maximizes the oracle at a finite time horizon, when relatively few noisy evaluations can be performed before the horizon. Our recursive, two-step lookahead expected payoff (r2LEY) acquisition function makes nonmyopic decisions at every stage by maximizing the estimated expected value of the oracle at the horizon. r2LEY circumvents the evaluation of the expensive multistep (more than two steps) lookahead acquisition function by recursively optimizing a two-step lookahead acquisition function at every stage; unbiased estimators of this latter function and its gradient are utilized for efficient optimization. r2LEY is shown to exhibit natural exploration properties far from the time horizon, enabling accurate emulation of the oracle, which is exploited in the final decision made at the horizon. To demonstrate the utility of r2LEY, we compare it with time-dependent extensions of popular myopic acquisition functions via both synthetic and real-world datasets.

1 Introduction

We consider the maximization of an expensive-to-evaluate oracle f with a finite budget of evaluations q . The inputs to f are \mathbf{x} , the *action* parameters from a compact domain $\mathcal{X} \subset \mathbb{R}^d$, and t , the *context* from a (possibly infinite) set of contexts \mathcal{T} . The observations $y \in \mathbb{R}$ made by observing f at the action-context pair (\mathbf{x}, t) are assumed to be corrupted by additive stochastic noise ϵ ; that is, $y = f(\mathbf{x}, t) + \epsilon$. Furthermore, we assume a context space \mathcal{T} whose members have a unique ordering (e.g., time), and we are interested in determining an optimum action at a given future context $T \in \mathcal{T}$ using only q evaluations of f . Such a problem fundamentally differs from general context-dependent k -armed bandit problems in that we are interested solely in the action that maximizes payoff at context $t = T$ as opposed to maximizing the *cumulative payoff* until T , as done by, for example, [10] and [19]. Additionally, we assume that only one observation can be made per context (hereafter “time”) t and that the schedule of observations $\{t_i\} \forall i = 1, \dots, q$ is given. The time-dependent maximization that we address arises, for example, in quantum computing applications [25] where, in order to find optimal tuning parameters \mathbf{x} at time T , quantum circuit parameters are tuned by using real-time noisy observations from the quantum device $f(\mathbf{x}, t)$.

The main challenges of our problem are the unknown structure of f and the high costs associated with each evaluation of $f(\mathbf{x}, t)$. Bayesian optimization (BO) [2; 18] with Gaussian process (GP) priors [17] suits the specific challenges posed by our problem, where observations at each round i , $y_i = f(\mathbf{x}_i, t_i) + \epsilon_i$, are made judiciously by leveraging information gained from previous observations, as a means of coping with the high costs of each observation. The key idea is to specify GP prior distributions on the oracle and the noise. That is, $f(\mathbf{x}, t) \sim \mathcal{GP}(0, k((\mathbf{x}, t), (\mathbf{x}', t')))$ and $\epsilon \sim \mathcal{GP}(0, \sigma_\epsilon^2)$, where k is a covariance function, σ_ϵ^2 is a constant noise variance and we assume that \mathcal{X} is a hypercube with lower and upper bounds lb and ub , respectively. Note that the covariance function captures the correlation between the observations in the (\mathbf{x}, t) space *jointly*; here we use the product composite form given by $k((\mathbf{x}, t), (\mathbf{x}', t')) = k_{\mathbf{x}}(\mathbf{x}, \mathbf{x}'; \theta_{\mathbf{x}}) \times k_t(t, t'; \theta_t)$, where $\theta_{\mathbf{x}}$ and θ_t parametrize the covariance functions for \mathbf{x} and t , respectively, and $\Omega = \{\theta_{\mathbf{x}}, \theta_t, \sigma_\epsilon^2\}$ are the unknown GP hyperparameters that are estimated from data by maximizing the marginal likelihood. The posterior predictive distribution of the output Y conditioned on available observations from the oracle, namely, $Y(\mathbf{x}, t | \mathcal{D}_n, \Omega) \sim \mathcal{GP}(\mu_n(\mathbf{x}, t), \sigma_n^2(\mathbf{x}, t))$, $\mathcal{D}_n = \{(\mathbf{x}_i, t_i), y_i\}_{i=1}^n$, is then used as a surrogate model for f . Note that μ_n and σ_n^2 are the posterior mean and variance of the GP, respectively, where the subscript n implies the conditioning based on n past observations. BO then proceeds by defining an *acquisition function* in terms of the GP posterior that is optimized in lieu of the expensive f to select the next point \mathbf{x}_{n+1} , and the process continues recursively until either the budget q is reached or the global maximum of the payoff function is realized; see Algorithm 1.

The standard acquisition functions in BO take a *greedy* or *myopic* approach, where each decision in the sequence is made as though it were the last, without accounting for the potential impact on the future decisions. Several greedy acquisition functions have been proposed, including the probability of improvement (PI) [11], the expected improvement (EI) [9; 13], and the GP upper confidence bound (UCB) [19]. Whereas in PI and EI the acquisition function is a probabilistic measure of *improvement* over a user-specified target, in UCB it is an optimistic estimate of the payoff. From a finite-budget BO perspective, such acquisition functions can be suboptimal [6] and moreover, optimizing them is guaranteed to attain the global optimum (under suitable regularity conditions) only in the limit $q \rightarrow \infty$, e.g., see [3; 21]. For finite-budget time-dependent optimization problems with a target time horizon T , an acquisition that seeks to optimize the *longsighted* decision at T is more appropriate. In other words, we want an approach that makes decisions at each t aimed at maximizing the payoff at T . Such finite-budget BO strategies are sometimes referred as *lookahead* approaches, since the current decision is made by looking ahead at future decisions.

In foundational work on finite-budget BO, Osborne [15] showed that proper Bayesian reasoning can be used to define an acquisition function where the $n+1$ th observation is made by marginalizing a loss function at the final (q th) observation, over all the remaining (\mathbf{x}_i, y_i) , $\forall i = n+2, \dots, q$ observations. However, the approach in [15] is restricted to a context-free setting and, furthermore, entailed defining the loss in terms of the best observed value, which, as we will show, does not apply to time-dependent problems. Another way to solve the finite-budget BO problem is to sequentially choose points that are most *informative* [4] about the global maximum/maximizer (or minimum/minimizer), e.g., see [7; 8; 22]. However, such information-theoretic approaches are known to involve an intractable form of the entropies, which often need an approximation and are tailored to seek a global optimum in a context-free setting (unlike our problem), and hence their suitability for time-dependent BO is unknown. Others have proposed *lookahead EI* in the context of finite-budget BO: Ginsbourger and Le Riche [5] showed that the lookahead EI is a dynamic program that chooses the EI maximizer in expectation, considering all possible strategies of the same budget. Our oracle changes with time and hence the improvement-based acquisition functions (e.g., EI and lookahead EI) do not suit our problem, since the appropriate target for a future t is unknown. A practical challenge with lookahead strategies is the computational tractability, as demonstrated in, for example, [5] and [15], which is partially mitigated by various approximation methods, e.g., [24; 12; 6]. In this work, we are interested in extending the finite-budget BO of [15] to time-dependent oracles (that is, where the best action depends on time), in addition to providing a practical solution to the tractability of the approach when looking ahead more than two steps.

Our main contributions are as follows: (i) We present the first strategy to solve the finite-budget BO for time-dependent problems. (ii) We replace the improvement-based acquisition function with the GP posterior (payoff) at T , with which we are able to obtain unbiased estimators for our acquisition function and its gradient, which can then be used in efficient gradient-based optimization methods. (iii) We improve the tractability of the multi-step lookahead problem by introducing a *recursive*

two-step lookahead strategy that looks ahead to T from the current step t ; we call our acquisition function Recursive Two-Step Lookahead Expected Payoff (r2LEY). (iv) We introduce software that implements r2LEY for solving time-dependent BO problems. (v) Finally, we establish the utility of our method by comparing it against a suite of existing BO acquisition functions on synthetic and real-world datasets.

Related work: Our approach is similar in spirit to the entropy-based approaches [7; 8; 22] in the sense that we make decisions that would maximize the expected payoff at T similarly to the way that those approaches make decisions that reduce uncertainty about the global maximum or maximizer. However, unlike the entropy-based approaches, our approach is able to generate realizations of analytically closed-form expressions that yield unbiased estimates of our acquisition function and its gradient. In the context of time-dependent BO, the only works we are aware of are [14] and [1]. We fundamentally differ from their approach in the following ways: (i) their goal is to track a time-varying optimum (ours is to predict it at T) and (ii) they don't address the finite-budget constraint as we do. Furthermore, setting $k_t(t_i, t_j) = (1 - \epsilon)^{|t_i - t_j|/2}$ (where ϵ is the *forgetting* factor as defined in [1]), our method is equivalent to [1] if we myopically make decisions at each t via UCB.

Algorithm 1: Generic Bayesian Optimization

```

1 Given:
2    $\mathcal{D}_n = \{\mathbf{x}_i, y_i\} \forall i = 1, \dots, n$ ,
3    $q$  total budget,
4   schedule  $\{t_{n+1}, \dots, t_q := T\}$ ,
5   and GP hyperparameters  $\Omega$ 
Result:  $(\mathbf{x}_T^*, y_T)$ 
6 for  $\ell = n + 1, \dots, q$ , do
7   Find  $\mathbf{x}_\ell^* = \underset{\mathbf{x} \in \mathcal{X}}{\operatorname{argmax}} \alpha(\mathbf{x}, t_\ell)$  (acquisition function)
8   Observe  $y_\ell = f(\mathbf{x}_\ell^*, t_\ell) + \epsilon_\ell$ 
9   Append  $\mathcal{D}_\ell = \mathcal{D}_{\ell-1} \cup \{(\mathbf{x}_\ell^*, y_\ell)\}$ 
10  Update GP hyperparameters  $\Omega$ 

```

2 r2LEY: Recursive two-step lookahead expected payoff acquisition function

Given n observations \mathcal{D}_n , let us define a function $I(\mathbf{x}, t)$ which implicitly depends on $Y_n(\mathbf{x}, t)$ and hence is a random variable. The one-step acquisition function to make the $n + 1$ th observation is then defined as

$$\alpha(\mathbf{x}, t_{n+1}) = \int_{Y_n} I(\mathbf{x}, t_{n+1}) p(Y_n(\mathbf{x}, t_{n+1}) | \mathcal{D}_n) dY_n. \quad (1)$$

Note that setting $I(\mathbf{x}, t_{n+1}) = (Y_n(\mathbf{x}, t_{n+1}) - \xi(t))^+$ leads to a time-dependent EI; see supplementary material for derivation. In the general EI setting, the target ξ is the best observed value, which does not suit time-dependent problems: We seek the maximizer of the payoff over $\mathbf{x} \in \mathcal{X}$ at $t = T$ as opposed to seeking the maximizer over the joint (\mathbf{x}, t) space. Choosing the target ξ as the maximum of the GP posterior mean—as in, for instance, [23]—involves an additional global optimization step just to determine ξ , which could be inaccurate.

Instead, we set the acquisition function to be the GP posterior at T , that is, $I(\mathbf{x}, t_{n+1}) = Y_n(\mathbf{x}, T)$. Essentially, at each stage, we make a decision that seeks the best payoff at T , our target time horizon. Note that in (1) and what follows, Y_n refers to the GP posterior conditioned on the past n observations and \mathbb{E}_n refers to the expectation taken with respect to Y_n .

Following (1), at the end of $i = q - 1$ rounds of the optimization, the (final) q th observation at $t_q := T$ is selected as the point that maximizes the mean of the GP posterior at time T . That is,

$$\begin{aligned}
\mathbf{x}_q^* &= \underset{\mathbf{x}_q \in \mathcal{X}}{\operatorname{argmax}} \int_{Y_{q-1}} Y_{q-1}(\mathbf{x}_q, T) p(Y_{q-1} | \mathcal{D}_{q-1}) dY_{q-1} \\
&= \underset{\mathbf{x}_q \in \mathcal{X}}{\operatorname{argmax}} \mathbb{E}_{q-1} Y_{q-1}(\mathbf{x}_q, T) \\
&= \underset{\mathbf{x}_q \in \mathcal{X}}{\operatorname{argmax}} \mu_{q-1}(\mathbf{x}_q, T),
\end{aligned} \quad (2)$$

where $p(Y_{q-1}|\mathcal{D}_{q-1})$ is the density of Y_{q-1} . Going back by one time-step to after $q-2$ observations of the oracle have been performed, the point \mathbf{x}_{q-1}^* is selected as follows.¹ Note that here, the $q-1$ th observation y_{q-1} is unknown and hence is drawn from the distribution $\mathcal{N}(\mu_{q-2}(\mathbf{x}, t_{q-1}), \sigma_{q-2}^2(\mathbf{x}, t_{q-1}))$ given whatever \mathbf{x} we choose to observe at t_{q-1} .

$$\mathbf{x}_{q-1}^* = \underset{\mathbf{x}_{q-1} \in \mathcal{X}}{\operatorname{argmax}} \int_{y_{q-1}} \left[\max_{\mathbf{x}_q \in \mathcal{X}} \mathbb{E}_{q-1} Y_{q-1}(\mathbf{x}_q, T) | \mathcal{D}_{q-2}, y_{q-1} \right] p(y_{q-1} | \mathbf{x}_{q-1}, \mathcal{D}_{q-2}) dy_{q-1}, \quad (3)$$

where, in (3), the inner maximization is with respect to \mathbf{x}_q and the outer maximization is with respect to \mathbf{x}_{q-1} . The above equation is written concisely as

$$\mathbf{x}_{q-1}^* = \underset{\mathbf{x}_{q-1} \in \mathcal{X}}{\operatorname{argmax}} \mathbb{E}_{q-2} \left[\max_{\mathbf{x}_q \in \mathcal{X}} \mathbb{E}_{q-1} Y_{q-1} | \mathcal{D}_{q-2}, y_{q-1} \right]. \quad (4)$$

Similarly, we could extend (4) to look ahead three steps to determine \mathbf{x}_{q-2}^* , which, however, would involve the marginalization of \mathbf{x}_{q-1} :

$$\mathbf{x}_{q-2}^* = \underset{\mathbf{x}_{q-2} \in \mathcal{X}}{\operatorname{argmax}} \int_{y_{q-2}} \int_{\mathbf{x}_{q-1}} \left[\max_{\mathbf{x}_q \in \mathcal{X}} \mathbb{E}_{q-1} Y_{q-1}(\mathbf{x}_q, T) | \mathcal{D}_{q-2}, y_{q-1} \right] p(y_{q-1} | \mathbf{x}_{q-1}, \mathcal{D}_{q-2}) p(\mathbf{x}_{q-1} | \mathcal{D}_{q-2}) d\mathbf{x}_{q-1} dy_{q-1}, \quad (5)$$

where $p(\mathbf{x}_{q-1} | \mathcal{D}_{q-2}) = p(\mathbf{x}_{q-1})$ can be set as $\mathcal{U}(lb, ub)$, where lb and ub are the lower and upper bounds of the domain \mathcal{X} . This additional step of marginalizing \mathbf{x}_{q-1} when moving from the two- to three-step lookahead makes the method computationally intractable, particularly as d increases. Using the same principle, one can define a generalized m -step lookahead to select \mathbf{x}_{q-m}^* by appropriately marginalizing all the remaining (\mathbf{x}_i, y_i) , $\forall i = q-m+1, \dots, q$. Instead, in this work, we recursively apply the two-step lookahead approach (4) to multi-step time-dependent BO problems (see Figure 1) and show how to efficiently optimize the two-step acquisition function defined as follows.

First, we write our two-step lookahead payoff acquisition function to select the $j+1$ th point—with $m = q-j$ observations remaining—as follows:

$$\begin{aligned} \alpha_{2LEY}(\mathbf{x}_{j+1}) &= \mathbb{E}_j \left[\max_{\mathbf{x}_q \in \mathcal{X}} \mu_{j+1}(\mathbf{x}_q, T) | y_{j+1}, \mathbf{x}_{j+1} \right] \\ &= \mathbb{E}_j \left[\max_{\mathbf{x}_q \in \mathcal{X}} g(\mathbf{x}_q, \mathbf{x}_{j+1}, T) \right], \end{aligned} \quad (6)$$

where $g(\mathbf{x}_q, \mathbf{x}_{j+1}, T) = \mu_{j+1}(\mathbf{x}_q, T) | y_{j+1}, \mathbf{x}_{j+1}$ and y_{j+1} is a draw from $\mathcal{N}(\mu_j(\mathbf{x}, t_{j+1}), \sigma_j^2(\mathbf{x}, t_{j+1}))$. Let $g^*(\mathbf{x}_{j+1}, T) = g(\mathbf{x}_q^*, T, \mathbf{x}_{j+1})$, where \mathbf{x}_q^* is a maximizer of $\mu_{j+1}(\mathbf{x}_q, T)$. Then the above equation can be written

$$\alpha_{2LEY}(\mathbf{x}_{j+1}) = \mathbb{E}_j [g^*(\mathbf{x}_{j+1}, T)]. \quad (7)$$

Note that in (7), it is implicit that $\alpha_{2LEY}(\mathbf{x}_{j+1})$ is the acquisition function to choose a point at t_{j+1} . The dependence of the right-hand side of (7) and the second line of (6) on \mathbf{x}_{j+1} can be seen by realizing that

$$g^*(\mathbf{x}_{j+1}, T) = \mu_{j+1}(\mathbf{x}_q^*, T) = \mathbf{k}_{j+1}^\top \mathbf{K}_{j+1}^{-1} \mathbf{y}_{j+1}, \quad (8)$$

where $\mathbf{k}_{j+1} = [k((\mathbf{x}_q^*, T), (\mathbf{x}_1, t_1)), \dots, k((\mathbf{x}_q^*, T), (\mathbf{x}_j, t_j)), k((\mathbf{x}_q^*, T), (\mathbf{x}_{j+1}, t_{j+1}))]^\top$. The expectation in (7) is not available in closed form, but can be approximated as

$$\alpha_{2LEY}(\mathbf{x}_{j+1}) = \mathbb{E}_j [g^*(\mathbf{x}_{j+1}, T)] \approx \frac{1}{M} \sum_{i=1}^M g^*(\mathbf{x}_{j+1}, T) | y_{j+1}^i \quad (9)$$

¹While \mathbf{x}_q^* is an estimate of the maximizer of f at t_q , \mathbf{x}_{q-1}^* is not an estimate of the maximizer of f at t_{q-1} . We use this notation to disambiguate the solution to the optimization problem in (3) from its decision variable \mathbf{x}_{q-1} .

The gradient of $g^*(\mathbf{x}_{j+1}, T)$ with respect to \mathbf{x}_{j+1} is given by

$$\begin{aligned}\nabla g^*(\mathbf{x}_{j+1}, T) &= \frac{\partial \mathbf{k}_{j+1}^\top}{\partial \mathbf{x}_{j+1}} \mathbf{K}_{j+1}^{-1} + \mathbf{k}_{j+1}^\top \frac{\partial \mathbf{K}_{j+1}^{-1}}{\partial \mathbf{x}_{j+1}} \\ &= \frac{\partial \mathbf{k}_{j+1}^\top}{\partial \mathbf{x}_{j+1}} \mathbf{K}_{j+1}^{-1} + \mathbf{k}_{j+1}^\top \mathbf{K}_{j+1}^{-1} \frac{\partial \mathbf{K}_{j+1}}{\partial \mathbf{x}_{j+1}} \mathbf{K}_{j+1}^{-1},\end{aligned}\quad (10)$$

where $\frac{\partial \mathbf{K}_{j+1}}{\partial \mathbf{x}_{j+1}}$ is a matrix of elementwise derivatives and the second line follows from a well-known lemma on the derivative of matrix inverse [17, p. 201–202]. With a continuously differentiable kernel $k(\cdot, \cdot)$ we state that

$$\nabla \alpha_{2LEY}(\mathbf{x}_{j+1}) = \nabla \mathbb{E}_j [g^*(\mathbf{x}_{j+1}, T)] = \mathbb{E}_j [\nabla g^*(\mathbf{x}_{j+1}, T)], \quad (11)$$

where the interchange of the gradient and expectation operators is via Theorem 3.1. Then the gradient is approximated as

$$\nabla \alpha_{2LEY}(\mathbf{x}_{j+1}) = \mathbb{E}_j [\nabla g^*(\mathbf{x}_{j+1}, T)] \approx \frac{1}{M} \sum_{i=1}^M g^*(\mathbf{x}_{j+1}, T) | y_{j+1}^i. \quad (12)$$

Furthermore, it can be shown (see Theorem 3.1) that (9) and (12) are unbiased estimators for α_{2LEY} and $\nabla \alpha_{2LEY}$, respectively. This gradient can then be used in a gradient-based optimizer to maximize our two-step lookahead acquisition function in an efficient manner. The overall algorithm is given by inserting the acquisition function obtained via Algorithm 2 into line 7 of Algorithm 1.

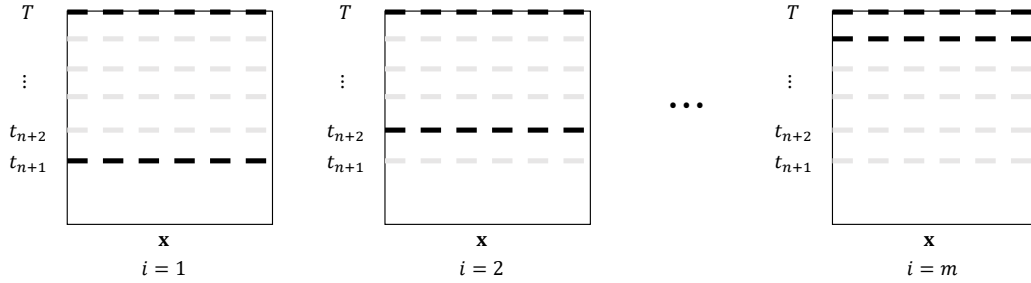


Figure 1: Recursive two-step lookahead method for time-dependent problems. Here, we start with n observations up to t_n and have m remaining observations to make, where $m + n = q$ (total budget).

Algorithm 2: Monte Carlo Approximation of (6) and (11)

- 1 **Given:** point \mathbf{x}_{j+1} , data $\mathcal{D}_j = \{(\mathbf{x}_i, t_i), y_i\} \forall i = 1, \dots, j$, and (simulation) budget M
 - Result:** estimate of α_{2LEY} and $\nabla \alpha_{2LEY}$
 - 2 **for** $i = 1, \dots, M$ **do**
 - 3 $y_{j+1}^i \sim \mathcal{N}(\mu_j, \sigma_j^2)$ (simulated y_{j+1})
 - 4 $\mathcal{D}_{j+1}^i = \mathcal{D}_j \cup \{(\mathbf{x}_{j+1}, y_{j+1}^i)\}$ (update data with simulation)
 - 5 $Y_{j+1}^i | \mathcal{D}_{j+1}^i \sim \mathcal{GP}(\mu_{j+1}^i, \sigma_{j+1}^{2,i})$ (update GP posterior)
 - 6 $\mathbf{x}_q^{*i} = \underset{\mathbf{x} \in \mathcal{X}}{\operatorname{argmax}} \mu_{j+1}^i(\mathbf{x}, \mathbf{x}_{j+1}, T)$ (maximizer of payoff at T)
 - 7 $\nu^i = \mu_{j+1}^{i*}(\mathbf{x}_{j+1}, T)$ (simulated acquisition function)
 - 8 $d\nu^i = \frac{\partial \mu_{j+1}^{i*}(\mathbf{x}_{j+1}, T)}{\partial \mathbf{x}_{j+1}}$ (simulated acquisition function gradient)
 - 9 **end**
 - 10 $\alpha_{2LEY} = \mathbb{E}_j [g^*(\mathbf{x}_{j+1}, T)] \approx \frac{1}{M} \sum_{i=1}^M \nu^i$
 - 11 $\nabla \alpha_{2LEY}(\mathbf{x}_{j+1}) = \mathbb{E}_j [\partial g^*(\mathbf{x}_{j+1}, T) / \partial \mathbf{x}_{j+1}] \approx \frac{1}{M} \sum_{i=1}^M d\nu^i$
-

3 Theoretical Properties

Theorem 3.1 (Interchange of gradient and expectation operators) *Let us write $g^*(\mathbf{x}_{j+1}, T) | y_{j+1}$ as $g^*(\mathbf{x}_{j+1}, T, y_{j+1})$ and, let \mathcal{Y} be the support of y_{j+1} , whose density is*

$p(y_{j+1})$, and suppose the domain of \mathbf{x}_{j+1} \mathcal{X} is an open set. Let $g^*(\mathbf{x}_{j+1}, T, y_{j+1})p(y_{j+1})$ and $\partial g^*(\mathbf{x}_{j+1}, T, y_{j+1})/\partial \mathbf{x}_{j+1}p(y_{j+1})$ be continuous on $\mathcal{X} \times \mathcal{Y}$. Suppose that there exist nonnegative functions $q_0(y_{j+1})$ and $q_1(y_{j+1})$ such that $|g^*(\mathbf{x}_{j+1}, T, y_{j+1})p(y_{j+1})| \leq q_0(y_{j+1})$ and $\|\frac{\partial g^*}{\partial \mathbf{x}_{j+1}}p(y_{j+1})\| \leq q_1(y_{j+1})$ for all $(\mathbf{x}_{j+1}, y_{j+1}) \in \mathcal{X} \times \mathcal{Y}$, where $\int_{\mathcal{Y}} q_1(y_{j+1})dy_{j+1} < \infty$ and $\int_{\mathcal{Y}} q_2(y_{j+1})dy_{j+1} < \infty$. Then,

$$\nabla \mathbb{E}_j [g^*(\mathbf{x}_{j+1}, T, y_{j+1})] = \mathbb{E}_j [\nabla g^*(\mathbf{x}_{j+1}, T, y_{j+1})]$$

Since $\nabla \alpha_{2LEY}(\mathbf{x}_{j+1}) = \mathbb{E}_j [\nabla g^*(\mathbf{x}_{j+1}, T, y_{j+1})]$, a realization of $\nabla g^*(\mathbf{x}_{j+1}, T, y_{j+1})$ yields an unbiased estimate of the true gradient.

See supplementary material for proof.

4 Experiments

The synthetic and real-world test data used in the experiments are described as follows. We introduce new synthetic test functions that can serve to benchmark general time-varying stochastic optimization problems.

Synthetic one-dimensional test functions: Each synthetic test function takes the form $f(\mathbf{x}, t) = f_{\mathbf{x}}(\mathbf{x}) + f_{\mathbf{x}t}(\mathbf{x}, t)$, where $f_{\mathbf{x}t}$ adds context dependence. For the one-dimensional cases, $f_{\mathbf{x}}(\mathbf{x}) = -4 \times (\mathbf{x} - 0.5)^2$ and $f_{\mathbf{x}t}$ is chosen to generate varying trajectories for \mathbf{x}^* at each t . The specific details are provided in the supplementary material and the contour plots of the payoff function are shown in Fig. 2. Notice that Quadratic c & d have exactly one local maximizer at every t whereas Quadratic b can be multimodal at specific t 's.

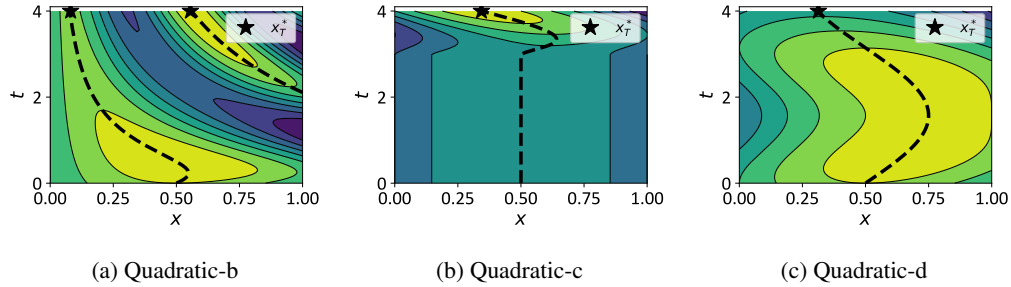


Figure 2: Contours that visualize the one-dimensional ($\mathcal{X} \subset \mathbb{R}$) time-dependent payoff function $f(\mathbf{x}, t)$. The dashed lines trace the location of \mathbf{x}^* at every t . We are interested in the maximizer of the payoff at T , \mathbf{x}_T^* . Each payoff function is generated by adding a nonlinear component (dependent on \mathbf{x} at t) to a simple one-dimensional quadratic function; see supplementary material for details.

Synthetic higher-dimensional test functions: For dimensions $d > 1$, various test functions are chosen for $f_{\mathbf{x}}(\mathbf{x})$, whereas $f_{\mathbf{x}t}$ is set to be that of Quadratic-d. The synthetic functions (for $f_{\mathbf{x}}(\mathbf{x})$) chosen are the Griewank (2d), Hartmann (3d), Hartmann (6d), Levy (8d), and Syblinski-Tang (10d); see [20] for details of each of these test functions.

Intel temperature sensor data: The following data are from sensor measurements from the Intel Berkeley Research Center, where 47 sensors are distributed in the building to measure various ambient air properties. We are specifically interested in the temperature data that are available as a time series for each sensor. We use the first 50 hours to train our model and predict the maximum temperature at $T = 100$.

SARCOS robot arm data: These data relates to an inverse dynamics problem for a SARCOS anthropomorphic robot arm with seven degrees of freedom. The original data have a 21-dimensional input space (7 joint positions, 7 joint velocities, 7 joint accelerations) and a 7-dimensional output space (joint torques). We use the first 7 of the 21 input variables as the \mathbf{x} , the 8th input variable as t and the first of the seven torques as output. The input t is scaled to range from $t = 0$ to $T = 4$ and the whole data is sorted (in ascending order) with respect to t . Data up to $t = 2$ are used as initial samples and the horizon is set as $T = 4$.

We start each experiment with $n = (d + 1) \times 20$ initial samples for test functions upto $d = 6$ and $n = (d + 1) \times 10$ for higher dimensions and, run our algorithm for $m = 10$ additional steps at fixed, equal time-steps. All initial samples span $0 \leq t \leq 2$ with one sample per time at equally spaced time-steps and the horizon is set at $T = 4$, unless otherwise mentioned. $M = 5000$ is set for all experiments and each experiment is repeated 20 times. Our metric for comparison is the \log_{10} normalized-simple-regret at T defined as $\log_{10} \frac{f_{max} - f(\mathbf{x}_T^*)}{f_{max} - f_{min}}$, where f_{max} and f_{min} are the maximum and minimum values for $f(\mathbf{x}, T) \forall \mathbf{x} \in \mathcal{X}$, and \mathbf{x}_T^* is the point selected by the algorithm at T . Both the mean (with standard errors) and median (with quantiles) values of the metric are compared across all experiments.

We compare our method against the most widely used myopic approaches in BO, namely the EI, PI, and UCB, which are modified appropriately for time-dependent problems (see supplementary material). EImumax and PImumax are the EI and PI, respectively with the target set as the maximum of the GP posterior mean at the current step, that is, $\mu_n(\mathbf{x}_{n+1}, t_{n+1})$, and the confidence parameter for UCB is set to 2. Additionally, we compare against a strategy that selects points uniformly at random from $\sim \mathcal{U}(lb, ub)$, where lb and ub are the lower and upper bounds of a hypercube. Additionally, we include R-EI, which is essentially Random except for the last evaluation, which is selected per EImumax.

4.1 Discussion

The metrics for all the numerical experiments, computed from 20 independent replications of each algorithm, are tabulated in Table 1. It is observed that the proposed r2LEY approach outperforms the other methods in terms of either the best average regret or the best worst-case regret. See the supplementary material for a more visual representation of these results.

The optimizer histories for the $d = 1$ (quadratic) test cases are shown in Figure 3, where each row represents a unique test function and each column represents one replication of r2LEY. In these figures, circles are the starting points and stars are the points chosen via r2LEY, and the black star is the final point at T . The contours in the background correspond to the true $f(\mathbf{x}, t)$. The points placed away from the yellow regions of the contours are indicative of the property of the method that it chooses locations of low immediate payoff to ultimately maximize the expected payoff at T . This property indirectly leads the algorithm to favor exploration away from T and exploitation at T , suiting our goal of maximizing the payoff solely at T . Among the three test functions in Figure 3, the Quadratic-b is particularly challenging because of the sharp gradients in the t direction; notice the sudden change in the location of the global maximum (around $t = 2$). Despite these challenges, the proposed approach is able to select the best payoff at T better than competing methods. In the case of Quadratic-b, the final point (black star) was always in the neighborhood of one of the two local maxima at T .

4.2 Computational Details

The benefits of the r2LEY are somewhat offset by the high computational costs relative to the other methods compared in this work. This cost mainly comes from the for loop in Algorithm 2, which includes $M = 5000$ computations of (1) GP posterior update with an additional observation, (2) GP posterior mean maximization and (3) the gradient computation of the acquisition function. However, these costs are mitigated in this work in the following ways. First, the covariance matrix inverse \mathbf{K}_n^{-1} is computed only once and stored, after which, with every new observation, updates to \mathbf{K}_n^{-1} are made to get \mathbf{K}_{n+1}^{-1} via the lemma in [16, p. 77]. This procedure reduces the computation from $\mathcal{O}(n + 1)^3$ to $\mathcal{O}(n + 1)^2$. Second, owing to the independence of each of the M computations in Algorithm 2, they are executed in parallel; in this regard we present a parallel implementation of r2LEY to be available upon publication. Third, the gradients of the acquisition function in r2LEY can be directly specified when analytically known. In other cases, the implementation of r2LEY takes advantage of automatic differentiation to compute gradients. Fourth, the maximization of the GP posterior mean is similarly solved efficiently with multistart gradient-based optimization. Finally, the GP hyperparameter updates are removed from the for loop and instead done only once per each of the m time-steps from t_n to T . With 72 processors, $M = 5000$ and $m = 1$, the current implementation takes approximately 3 minutes of wall-clock time to execute one instance of r2LEY.

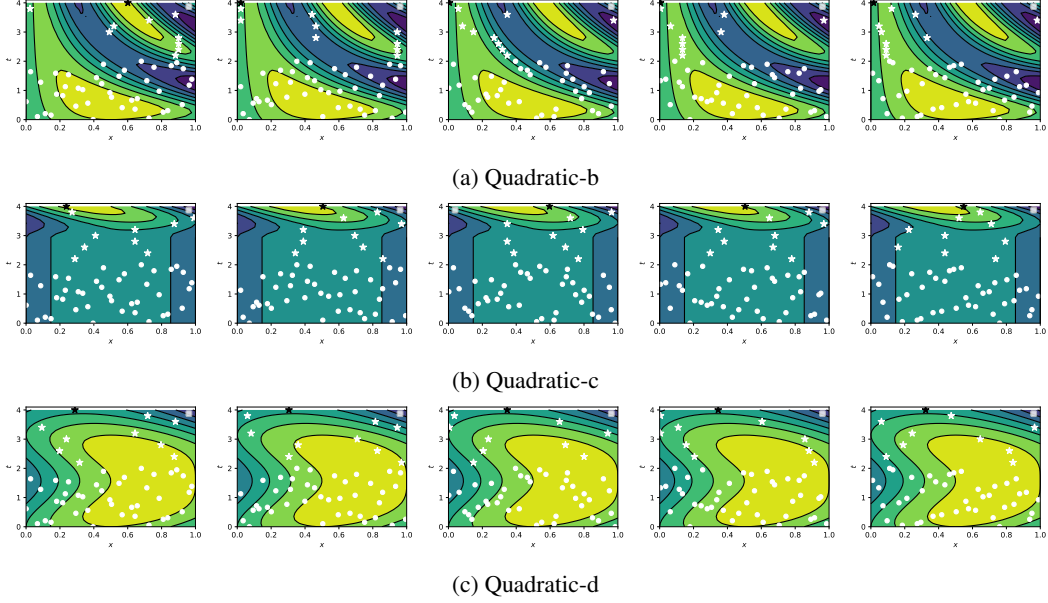


Figure 3: Performance of the proposed approach on the 1d problems for 5 repetitions (left to right). Circles are initial samples, stars are points selected by r2LEY and the black star is the final point \mathbf{x}_T^* . Contours represent the *true* noise-free payoff function for reference.

Test Case	d	$\log_{10}[\text{normalized simple regret}]$					
		EImumax	PIumax	UCB	Random	R-EI	r2LEY
Quad-b	1	-0.32 ± 0.04	-0.47 ± 0.03	-0.50 ± 0.17	-0.31 ± 0.08	-0.48 ± 0.09	-0.55 ± 0.06
Quad-c	1	-0.57 ± 0.03	-0.93 ± 0.14	-0.89 ± 0.16	-1.26 ± 0.24	-0.90 ± 0.08	-0.94 ± 0.07
Quad-d	1	-1.45 ± 0.25	-2.06 ± 0.16	-1.29 ± 0.16	-1.41 ± 0.27	-0.94 ± 0.08	-3.63 ± 0.27
Gri	2	-0.77 ± 0.04	-0.67 ± 0.04	-0.85 ± 0.042	-0.32 ± 0.04	-0.35 ± 0.04	-1.00 ± 0.05
Hart3	3	-0.37 ± 0.08	-0.33 ± 0.07	-0.46 ± 0.13	-0.51 ± 0.11	-0.75 ± 0.12	-3.59 ± 0.39
Hart6	6	-0.41 ± 0.06	-0.37 ± 0.02	-0.29 ± 0.04	-0.34 ± 0.03	-0.52 ± 0.03	-3.31 ± 0.46
Levy8	8	-0.35 ± 0.02	-0.35 ± 0.02	-0.48 ± 0.04	-0.34 ± 0.01	-0.32 ± 0.02	-1.21 ± 0.59
St-Ta	10	-0.33 ± 0.02	-0.32 ± 0.02	-0.41 ± 0.04	-0.34 ± 0.02	-0.32 ± 0.01	-0.65 ± 0.02
Intel	2	-0.36 ± 0.04	-0.27 ± 0.04	-0.58 ± 0.05	-0.45 ± 0.05	-0.31 ± 0.05	-1.24 ± 0.35
SARCOS	7	-0.40 ± 0.04	-0.35 ± 0.06	-0.31 ± 0.03	-0.40 ± 0.05	-0.48 ± 0.07	-2.52 ± 0.34

Table 1: Mean \pm standard error of $\log_{10}[\text{normalized simple regret}]$ at T . Larger fonts represent best method in terms of either mean regret or worst-case regret. Each algorithm is repeated 20 times with independent starting samples to compute metric.

5 Conclusions

Optimization of a time-dependent expensive stochastic oracle finds application in a variety of fields including quantum computing, finance, power & energy systems and aerospace engineering. In this work, we specifically address problems where the best decision at a finite time horizon is of interest, given a finite budget of evaluations. Our proposed approach extends the lookahead approach in BO to time-dependent problems. We overcome the tractability issue of multi-step lookahead approaches by recursively solving a two-step lookahead problem where, at each step, we look ahead at the desired time horizon. Furthermore, we solve the optimization of our acquisition function efficiently by computing unbiased estimators of its gradient. Demonstrations with synthetic and real-world datasets revealed that our approach leads to the best average and worst-case regret compared to competing methods.

Broader impact statement

Our proposed method is motivated by the need for optimal decision making in the presence *limited* and *uncertain* information. For example, measuring output of physical or computer experiments governing complex systems can be biased, noisy and involve costs that make querying them more than just a few dozen times prohibitively expensive. Tuning a quantum device is a prime example, but one may also think of other applications such as measuring the aerosturcutural performance of a prototype aircraft in a windtunnel, which involves sophisticated instrumentation and an expensive setup. In such situations, reliable decision making is critical and involve high stakes and yet is faced with the challenge of limited information. We discuss theoretical developments that has the aforementioned broader impact.

References

- [1] Ilija Bogunovic, Jonathan Scarlett, and Volkan Cevher. Time-varying Gaussian process bandit optimization. In *Proceedings of the 19th International Conference on Artificial Intelligence and Statistic*, pages 314–323, 2016.
- [2] Eric Brochu, Vlad M. Cora, and Nando De Freitas. A tutorial on Bayesian optimization of expensive cost functions, with application to active user modeling and hierarchical reinforcement learning. *arXiv:1012.2599*, 2010.
- [3] Adam D. Bull. Convergence rates of efficient global optimization algorithms. *Journal of Machine Learning Research*, 12:2879–2904, 2011.
- [4] Thomas M. Cover and Joy A. Thomas. *Elements of Information Theory*. John Wiley & Sons, 2012.
- [5] David Ginsbourger and Rodolphe Le Riche. Towards Gaussian process-based optimization with finite time horizon. In *Contributions to Statistics*, pages 89–96. Springer, 2010.
- [6] Javier Gonzalez, Michael Osborne, and Neil Lawrence. GLASSES: Relieving the myopia of Bayesian optimisation. volume 51 of *Proceedings of Machine Learning Research*, pages 790–799, 2016.
- [7] Philipp Hennig and Christian J. Schuler. Entropy search for information-efficient global optimization. *Journal of Machine Learning Research*, 13(Jun):1809–1837, 2012.
- [8] José Miguel Hernández-Lobato, Matthew W. Hoffman, and Zoubin Ghahramani. Predictive entropy search for efficient global optimization of black-box functions. In *Advances in Neural Information Processing Systems*, pages 918–926, 2014.
- [9] Donald R. Jones, Matthias Schonlau, and William J. Welch. Efficient global optimization of expensive black-box functions. *Journal of Global Optimization*, 13(4):455–492, 1998.
- [10] Andreas Krause and Cheng S. Ong. Contextual Gaussian process bandit optimization. In *Advances in Neural Information Processing Systems*, pages 2447–2455, 2011.
- [11] Harold J. Kushner. A new method of locating the maximum point of an arbitrary multipeak curve in the presence of noise. *Journal of Basic Engineering*, 86(1):97–106, 1964.
- [12] Remi Lam, Karen Willcox, and David H. Wolpert. Bayesian optimization with a finite budget: An approximate dynamic programming approach. In *Advances in Neural Information Processing Systems*, pages 883–891, 2016.
- [13] Jonas Mockus, Vytautas Tiešis, and Antanas Žilinskas. The application of Bayesian methods for seeking the extremum. *Towards Global Optimization*, 2:117–129, 1978.
- [14] Favour M. Nyikosa, Michael A. Osborne, and Stephen J. Roberts. Bayesian optimization for dynamic problems. *arxiv.org/1803.03432*, 2018.
- [15] Michael A. Osborne. *Bayesian Gaussian Processes for Sequential Prediction, Optimisation and Quadrature*. PhD thesis, Oxford University, UK, 2010.

- [16] William H. Press, Saul A. Teukolsky, William T. Vetterling, and Brian P. Flannery. *Numerical Recipes in C++*. Cambridge University Press, 2nd edition, 2002.
- [17] C. E. Rasmussen and C. K. I. Williams. *Gaussian Processes for Machine Learning*. MIT Press, 2006.
- [18] Bobak Shahriari, Kevin Swersky, Ziyu Wang, Ryan P. Adams, and Nando De Freitas. Taking the human out of the loop: A review of Bayesian optimization. *Proceedings of the IEEE*, 104(1):148–175, 2015.
- [19] Niranjan Srinivas, Andreas Krause, Sham M. Kakade, and Matthias Seeger. Gaussian process optimization in the bandit setting: No regret and experimental design. In *Proceedings of the International Conference on Machine Learning*, 2009.
- [20] S. Surjanovic and D. Bingham. Virtual library of simulation experiments: Test functions and datasets. Retrieved May 23, 2020, from <http://www.sfu.ca/~ssurjano>.
- [21] Emmanuel Vazquez and Julien Bect. Convergence properties of the expected improvement algorithm with fixed mean and covariance functions. *Journal of Statistical Planning and Inference*, 140(11):3088–3095, 2010.
- [22] Zi Wang and Stefanie Jegelka. Max-value entropy search for efficient Bayesian optimization. In *Proceedings of the 34th International Conference on Machine Learning*, volume 70, pages 3627–3635, 2017.
- [23] Ziyu Wang and Nando de Freitas. Theoretical analysis of Bayesian optimisation with unknown Gaussian process hyper-parameters. *arXiv:1406.7758*, 2014.
- [24] Jian Wu and Peter Frazier. Practical two-step lookahead Bayesian optimization. In *Advances in Neural Information Processing Systems*, pages 9810–9820, 2019.
- [25] D. Zhu, N. M. Linke, M. Benedetti, K. A. Landsman, N. H. Nguyen, C. H. Alderete, A. Perdomo-Ortiz, N. Korda, A. Garfoot, C. Brecque, L. Egan, O. Perdomo, and C. Monroe. Training of quantum circuits on a hybrid quantum computer. *Science Advances*, 5(10):eaaw9918, 2019.

Time-Dependent Acquisition Functions

We present the following time-dependent extensions of existing acquisition functions namely, the EI, PI and UCB.

Expected Improvement

The improvement function is defined as

$$I(\mathbf{x}, t) = \max(0, Y(\mathbf{x}, t) - \xi), \quad (13)$$

where ξ is the target. Then $I(\mathbf{x}, t) \sim \mathcal{N}((\mu(\mathbf{x}, t) - \xi)^+, \sigma^2(\mathbf{x}, t))$. So

$$\alpha_{\text{EI}}(\mathbf{x}, t) := \mathbb{E}_Y(I) = \int_{I=0}^{\infty} I \left\{ \frac{1}{\sqrt{2\pi}\sigma(\mathbf{x}, t)} \exp \left[-\frac{(I - Y(\mathbf{x}, t) + \xi)^2}{2\sigma^2(\mathbf{x}, t)} \right] dI \right\} \quad (14)$$

where the lower limit in the above integral is zero due to the fact that the improvement is non-negative. Further simplification can be obtained via transformation of variable as

$$u = \frac{I - Y + \xi}{\sigma}$$

which transforms the integral in (14) as

$$\begin{aligned} \alpha_{\text{EI}}(\mathbf{x}, t) &= \int_{u=\frac{\xi-Y}{\sigma}}^{\infty} (\sigma u + Y - \xi) \frac{1}{\sqrt{2\pi}} \exp(-u^2/2) du \\ &= \frac{1}{\sqrt{2\pi}} \int_{u=\frac{\xi-Y}{\sigma}}^{\infty} \sigma u \exp(-u^2/2) du + \frac{1}{\sqrt{2\pi}} (Y - \xi) \int_{u=\frac{\xi-Y}{\sigma}}^{\infty} \exp(-u^2/2) du \\ &= \frac{1}{\sqrt{2\pi}} [\sigma(-\exp(-u^2/2))]_{\frac{\xi-Y}{\sigma}}^{\infty} + \frac{1}{\sqrt{2\pi}} (Y - \xi) \int_{u=\frac{\xi-Y}{\sigma}}^{\infty} \exp(-u^2/2) du \end{aligned} \quad (15)$$

By denoting the standard normal pdf and cdf as $\phi()$ and $\Phi()$ respectively, the above equation can be re-written concisely as

$$\alpha_{\text{EI}}(\mathbf{x}, t) = \sigma(\mathbf{x}, t) \Phi \left(\frac{\xi - \mu}{\sigma} \right) + (\mu - \xi) \phi \left(\frac{\xi - \mu}{\sigma} \right) \quad (16)$$

Note that for time-dependent problems, where the oracle is changing with time, it is required that $\xi = \xi(t)$.

GP Upper Confidence Bound

The GP-UCB for time-dependent oracles is specified as an optimistic estimate of the posterior GP mean as follows

$$\alpha_{\text{UCB}}(\mathbf{x}, t) = \mu(\mathbf{x}, t) + \beta^{1/2} \sigma(\mathbf{x}, t), \quad (17)$$

Probability of Improvement

The PI acquisition function for time-dependent oracles is given as follows

$$\begin{aligned} \alpha_{\text{PI}}(\mathbf{x}, t) &= P(Y(\mathbf{x}, t) \geq \xi) \\ &= \Phi \left(\frac{\mu(\mathbf{x}, t) - \xi}{\sigma(\mathbf{x})} \right), \end{aligned} \quad (18)$$

where as in EI, the target $\xi = \xi(t)$ for time-dependent problems.

1D Quadratic Test Functions

We first consider quadratic 1D functions f over the domain $\mathcal{X} = [0, 1]$ with

$$f_{\mathbf{x}}(\mathbf{x}) = -\alpha \times (\mathbf{x} - s)^2, \quad (19)$$

where s and α are scalar parameters. The context-dependent component takes the three forms

$$\text{Quadratic-a : } f_{\mathbf{x}t} = \sin(\pi(\mathbf{x} + t)) + \cos(\pi(\mathbf{x} + t))$$

$$\text{Quadratic-b : } f_{\mathbf{x}t} = \sin(\pi(\mathbf{x}t)) + \cos(\pi(\mathbf{x}t))$$

$$\text{Quadratic-c : } f_{\mathbf{x}t} = \sin(\pi(\mathbf{x}[t - 3]^+)) + \cos(\pi(\mathbf{x}[t - 3]^+))$$

$$\text{Quadratic-d : } f_{\mathbf{x}t} = 2\mathbf{x}\sin(t) - \sin^2(t),$$

where, $[t - 3]^+ \equiv \max(0, t - 3)$ is specified to induce movement of \mathbf{x}_t^* for $t \geq 3$. The different $f_{\mathbf{x}t}$ functions are chosen to create varying patterns of context-dependent \mathbf{x}_t^* . In (19), we set $s = 0.5, \alpha = 4.0$; see Figure 4 for further details.

Details of synthetic test functions

Table 2: Domain and maximizer of the time-independent part of the synthetic test functions. Note that each test function is composed of a time-dependent component $f_{\mathbf{x}t}$ (not included in the table) that moves the maximizer with respect to t in the experiments

Test case	d	\mathcal{X}	\mathcal{T}	$\operatorname{argmax}_{\mathbf{x} \in \mathcal{X}} f_{\mathbf{x}}(\mathbf{x})$
Quadratic-a	1	$[0, 1]$	$[0, 4]$	0.5
Quadratic-b	1	$[0, 1]$	$[0, 4]$	0.5
Quadratic-c	1	$[0, 1]$	$[0, 4]$	0.5
Quadratic-d	1	$[0, 1]$	$[0, 4]$	0.5
Griewank	2	$[-5, 5]^2$	$[0, 4]$	$[0, 0]$
Hartmann-3d	3	$[0, 1]^3$	$[0, 4]$	$[0.11, 0.56, 0.85]$
Hartmann-6d	6	$[0, 1]^6$	$[0, 4]$	$[0.20, 0.15, 0.48, 0.28, 0.31, 0.66]$
Levy	8	$[-10, 10]^8$	$[0, 4]$	$[1, \dots, 1]$
Styblinski-Tang	10	$[-5, 5]^{10}$	$[0, 4]$	$[-2.903534, \dots, -2.903534]$
Intel Sensor	2	$[0.5, 40.5]^2$	$[0, 100]$	-
SARCOS Robot	7	$[0, 2]^7$	$[0, 4]$	-

Proof of Theorem 3.1

Theorem 5.1 (Interchange of gradient and expectation operators) *Let us write $g^*(\mathbf{x}_{j+1}, T)|_{y_{j+1}}$ as $g^*(\mathbf{x}_{j+1}, T, y_{j+1})$ and, let \mathcal{Y} be the support of y_{j+1} , whose density is $p(y_{j+1})$, and the domain of \mathbf{x}_{j+1} be \mathcal{X} . Let $g^*(\mathbf{x}_{j+1}, T, y_{j+1}) \times p(y_{j+1})$ and $\partial g^*(\mathbf{x}_{j+1}, T, y_{j+1})/\partial \mathbf{x}_{j+1} \times p(y_{j+1})$ be continuous on $\mathcal{X} \times \mathcal{Y}$. Furthermore, assume that the kernel $k(\cdot)$ is continuously differentiable in \mathcal{X} . Suppose that there exist nonnegative functions $q_0(y_{j+1})$ and $q_1(y_{j+1})$ such that $|g^*(\mathbf{x}_{j+1}, T, y_{j+1}) \times p(y_{j+1})| \leq q_0(y_{j+1})$ and $\|\partial g^*/\partial \mathbf{x}_{j+1} \times p(y_{j+1})\| \leq q_1(y_{j+1})$ for all $(\mathbf{x}_{j+1}, y_{j+1}) \in \mathcal{X} \times \mathcal{Y}$, where $\int_{\mathcal{Y}} q_1(y_{j+1}) dy_{j+1} < \infty$ and $\int_{\mathcal{Y}} q_2(y_{j+1}) dy_{j+1} < \infty$. Then,*

$$\nabla \mathbb{E}_j [g^*(\mathbf{x}_{j+1}, T, y_{j+1})] = \mathbb{E}_j [\nabla g^*(\mathbf{x}_{j+1}, T, y_{j+1})]$$

Since $\nabla \alpha_{2LEY}(\mathbf{x}_{j+1}) = \mathbb{E}_j [\nabla g^*(\mathbf{x}_{j+1}, T, y_{j+1})]$, a realization of $\nabla g^*(\mathbf{x}_{j+1}, T, y_{j+1})$ yields an unbiased estimate of the true gradient.

In what follows, we use $g^*(\mathbf{x}_{n+1})$ to denote $g^*(\mathbf{x}_{n+1}, T, y_{n+1})$ for the sake of brevity

$$\begin{aligned} \frac{\partial}{\partial \mathbf{x}_{n+1}} \mathbb{E}_n [g^*(\mathbf{x}_{n+1})] &= \lim_{h \rightarrow 0} \frac{1}{h} \{ \mathbb{E}_n [g^*(\mathbf{x}_{n+1} + h)] - \mathbb{E}_n [g^*(\mathbf{x}_{n+1})] \} \\ &= \lim_{h \rightarrow 0} \left\{ \mathbb{E}_n \frac{1}{h} [g^*(\mathbf{x}_{n+1} + h) - g^*(\mathbf{x}_{n+1})] \right\} \\ &= \lim_{h \rightarrow 0} \left\{ \mathbb{E}_n \frac{\partial g^*(\bar{\mathbf{x}}_{n+1})}{\partial \mathbf{x}_{n+1}} \right\}, \end{aligned} \quad (20)$$

where, $\bar{\mathbf{x}}_{n+1} = \lambda \mathbf{x}_{n+1} + (1 - \lambda)(\mathbf{x}_{n+1} + h)$ for some $\lambda \in [0, 1]$ and the last line follows from the first order mean-value theorem by assuming (but proven below) that $\nabla g^*(\mathbf{x}_{n+1})$ exists and is continuous in \mathcal{X} .

Finally, we bring the limit inside the integral by the Lebesgue's dominated convergence theorem and state

$$\frac{\partial}{\partial \mathbf{x}_{n+1}} \mathbb{E}_n [g^*(\mathbf{x}_{n+1})] = \left\{ \mathbb{E}_n \lim_{h \rightarrow 0} \frac{\partial g^*(\bar{\mathbf{x}}_{n+1})}{\partial \mathbf{x}_{n+1}} \right\} = \mathbb{E}_n \frac{\partial g^*(\mathbf{x}_{n+1})}{\partial \mathbf{x}_{n+1}}. \quad (21)$$

To prove that $g^*(\mathbf{x}_{j+1}, T, y_{j+1}) \times p(y_{j+1})$ and $\partial g^*(\mathbf{x}_{j+1}, T, y_{j+1})/\partial \mathbf{x}_{j+1} \times p(y_{j+1})$ are continuous on $\mathcal{X} \times \mathcal{Y}$, first note that $y_{n+1} \sim \mathcal{N}(\mu_{n+1}, \sigma_{n+1}^2)$ and hence its density $p(y)$ is continuous in \mathcal{Y} owing to its exponential structure.

Consider the expansion of g^* and ∇g^* repeated below

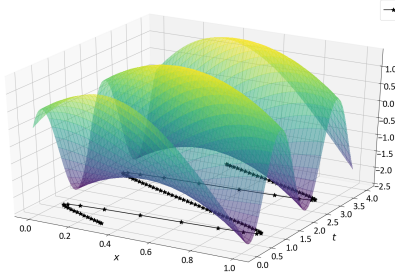
$$g^*(\mathbf{x}_{n+1}, T) = \mathbf{k}_{n+1}^\top \mathbf{K}_{n+1}^{-1} \mathbf{y}_{n+1}, \quad (22)$$

$$\nabla g^*(\mathbf{x}_{n+1}, T) = \frac{\partial \mathbf{k}_{n+1}^\top}{\partial \mathbf{x}_{n+1}} \mathbf{K}_{n+1}^{-1} + \mathbf{k}_{n+1}^\top \mathbf{K}_{n+1}^{-1} \frac{\partial \mathbf{K}_{n+1}}{\partial \mathbf{x}_{n+1}} \mathbf{K}_{n+1}^{-1}. \quad (23)$$

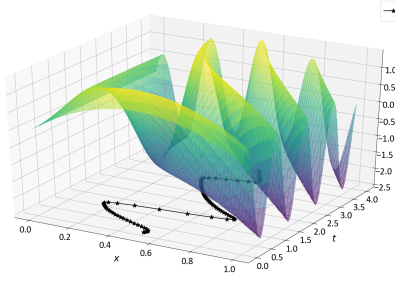
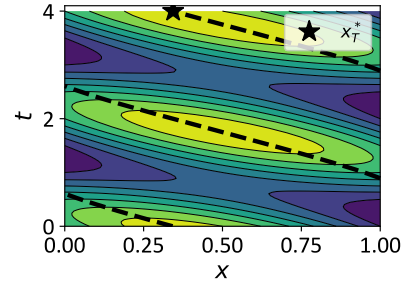
Since each element of \mathbf{k}_{n+1} is the output of a continuously differentiable kernel (by assumption), \mathbf{k}_{n+1} is continuously differentiable in \mathcal{X} . Similarly, due to the differentiability of the kernel, \mathbf{K}_{n+1} is continuously differentiable and so is its inverse. Since the product of continuous functions is continuous, $g^*(\mathbf{x}_{n+1})$ is continuous in \mathcal{X} . By the same arguments and by the fact that the elementwise derivative in $\frac{\partial \mathbf{K}_{n+1}}{\partial \mathbf{x}_{n+1}}$ is continuous, ∇g^* is also continuous in \mathcal{X} .

Finally, since products of continuous functions are continuous, the products $g^*(\mathbf{x}_{n+1}, y_{n+1})p_{\mathcal{Y}}(y_{n+1})$ and $\partial g^*(\mathbf{x}_{n+1}, y_{n+1})/\partial \mathbf{x}_{n+1} p_{\mathcal{Y}}(y_{n+1})$ are continuous on $\mathcal{X} \times \mathcal{Y}$. Therefore (21) holds. \square

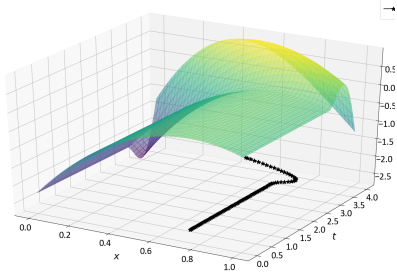
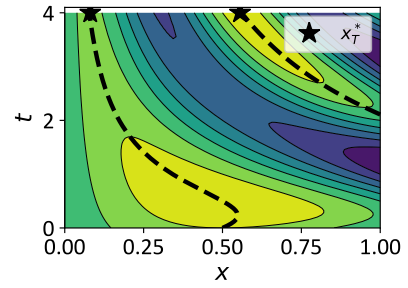
Experiments



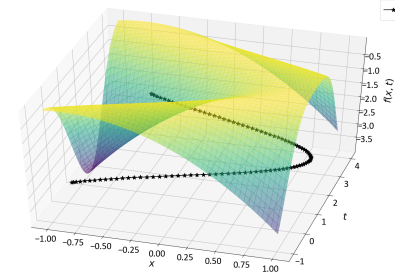
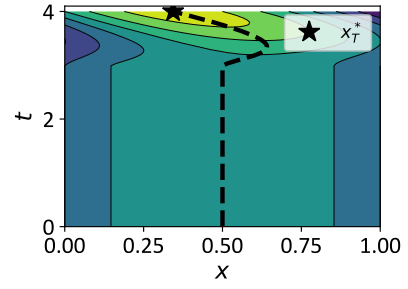
(a) Quadratic-a



(b) Quadratic-b



(c) Quadratic-c



(d) Quadratic-d

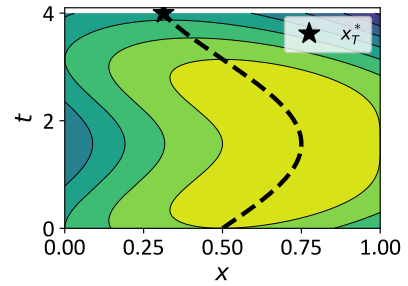
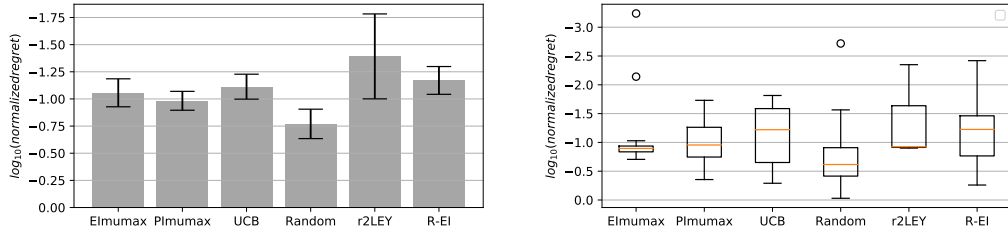
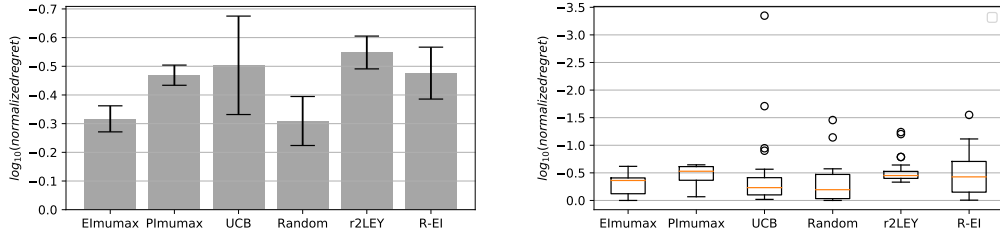


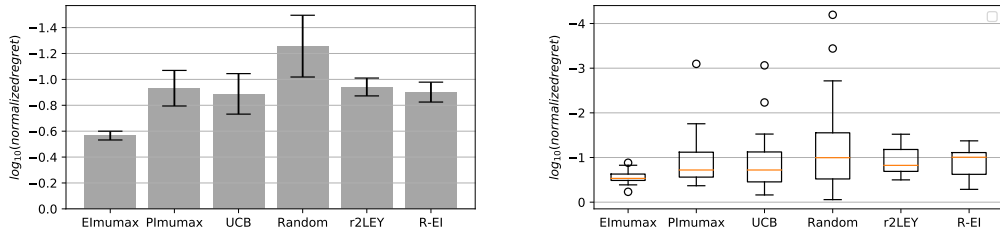
Figure 4: Quadratic ($d = 1$) test cases. Dashed lines in the contour plots represent trajectory of local maximizer. Notice that in Quadratic-a, the maximizer makes sudden jumps (from one boundary to other) at around $t = 1$ and $t = 3$ and, Quadratic-b has two local maxima starting $t = 2$.



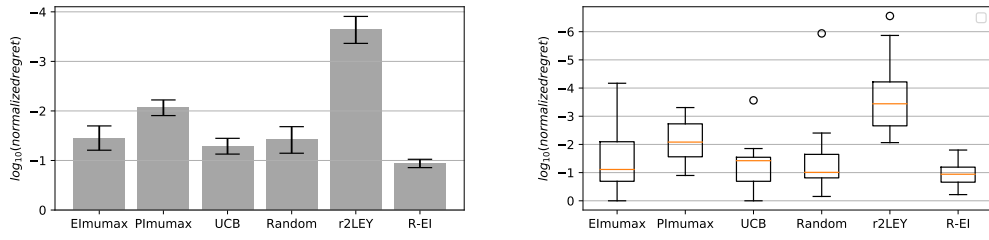
(a) Quadratic-a



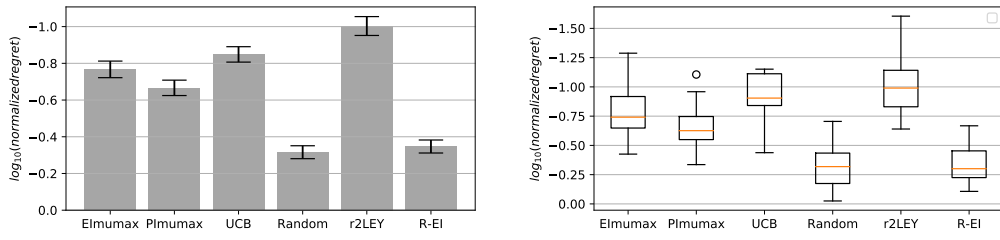
(b) Quadratic-b



(c) Quadratic-c

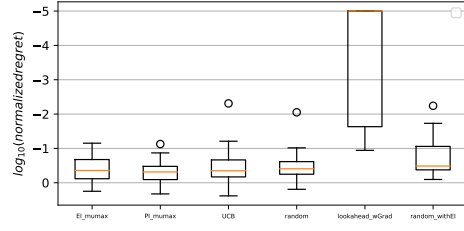
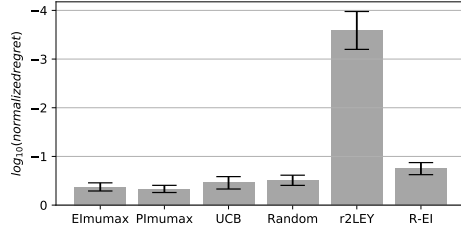


(d) Quadratic-d

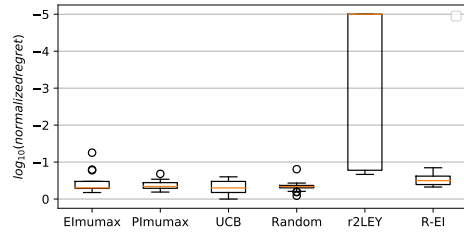
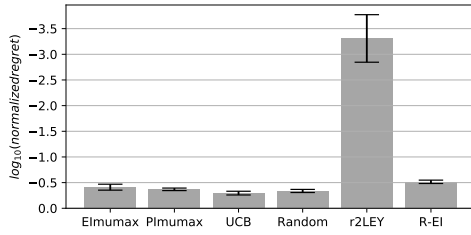


(e) Griewank-2d

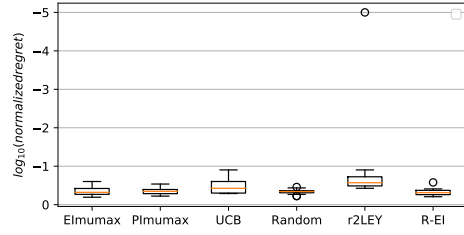
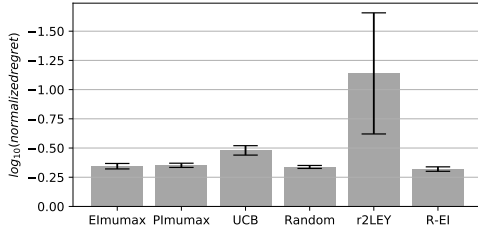
Figure 5



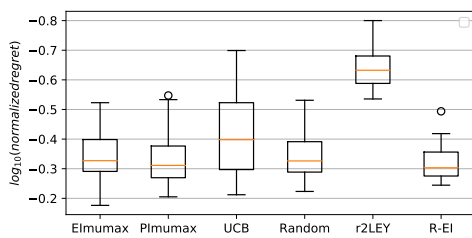
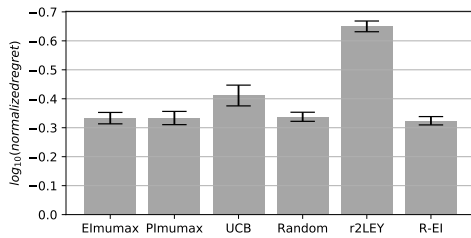
(f) Hartmann-3d



(g) Hartmann-6d

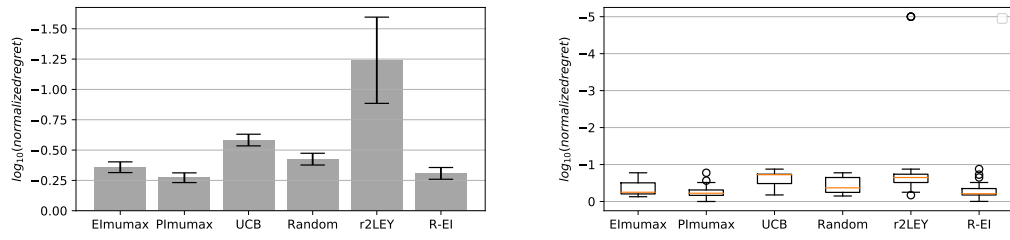


(h) Levy-8d

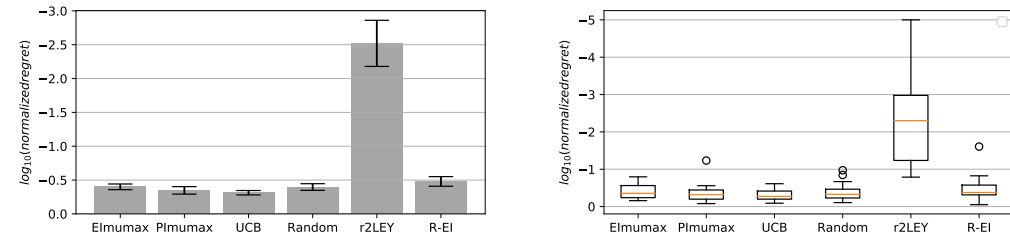


(i) Styblinski-Tang-10d

Figure 5



(j) Intel Sensor



(k) SARCOS Robot

Figure 5: \log_{10} [normalized simple regret] at T for all the experiments. Left column are mean \pm std. error.